

HALO: Learning to Prune Neural Networks with Shrinkage

Skyler Seto, Martin T. Wells and Wenyu Zhang
 Department of Statistics and Data Science
 Cornell University
 Ithaca, NY
 {ss3349, mtw1, wz258}@cornell.edu

Abstract

Deep neural networks achieve state-of-the-art performance in a variety of tasks by extracting a rich set of features from unstructured data, however this performance is closely tied to model size. Modern techniques for inducing sparsity and reducing model size are (1) network pruning, (2) training with a sparsity inducing penalty, and (3) training a binary mask jointly with the weights of the network. We study different sparsity inducing penalties from the perspective of Bayesian hierarchical models and present a novel penalty called **H**ierarchical **A**daptive **L**asso (HALO) which learns to adaptively sparsify weights of a given network via trainable parameters. When used to train over-parametrized networks, our penalty yields small subnetworks with high accuracy without fine-tuning. Empirically, on image recognition tasks, we find that HALO is able to learn highly sparse network (only 5% of the parameters) with significant gains in performance over state-of-the-art magnitude pruning methods at the same level of sparsity. Code is available at <https://github.com/skyler120/sparsity-halo>.

Keywords: Deep Learning, Feature Selection, Penalization, Pruning

1 Introduction

Machine learning systems have improved many modern technologies including web search systems, recommendation systems, and cameras. Traditional machine learning systems rely on human experts to extract features from the raw data in order to perform classification. As such, these systems are limited by the features that humans design. Representation learning in contrast is a method for automatically discovering relevant features from the raw data for classification.

Deep neural networks (DNNs) are representation learning methods that learn representations of data by composing non-linear functions that transform the input through a series of compositions. With enough composi-

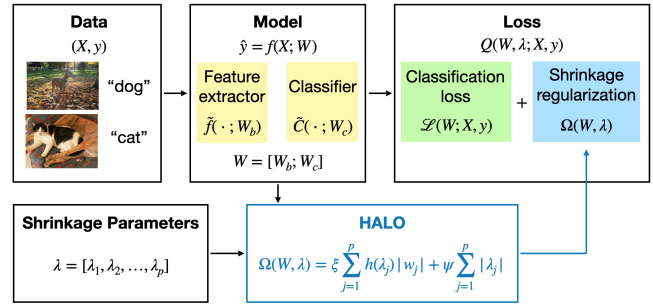


Figure 1: Overview of HALO: we perform MAP estimation of our Bayesian hierarchical model by appending an additional penalty to the standard loss function which enforces sparsity via shrinkage on the parameters of the network.

tions, these deep learning systems can model arbitrarily complex functions. For example, a convolutional neural network operating on images learns features by taking the raw image and applies a series of convolutions over patches of the image to generate spatial features. In a convolutional neural network, the learned features in the first layer may be edge detectors, in the second layer may detect arrangements of edges, and in the third layer recognize basic objects [33]. As the deep neural network is trained for a specific task (such as image classification) the features obtained in the later layers of the network become more specialized for the task.

Due to their ability to extract complex feature representations, neural networks have achieved state-of-the-art performance on numerous problems in image recognition [31], speech recognition [27], natural language understanding [14], and healthcare [15]. However, this impressive performance is closely tied to model size, since DNNs rely on compositions of numerous non-linear functions to extract features and will often contain millions of parameters. As such, in settings where memory footprint and computational efficiency are important such as on low-power devices, DNNs although favored

over smaller models with limited performance are unable to be deployed.

In this work, we propose a method to learn sparse neural networks that match the performance of over-parametrized networks with little performance reduction. We motivate our approach as a Bayesian hierarchical model which adaptively shrinks the weights of a network. We derive the MAP estimate for this model and call this penalty **Hierarchical Adaptive Lasso** (HALO). HALO regularizes model parameters in a hierarchical fashion and shrinks each model parameter based on its importance to the data and model. With the resulting order in the magnitude of the model parameters, further pruning by simple thresholding can be applied to obtain the desired level of sparsity with less drop in accuracy than competing methods. We demonstrate on multiple image recognition tasks and neural network architectures that HALO is able to learn highly sparse feature extractors with little to no accuracy drop. An overview of the additions we make to the standard training pipeline is provided in Figure 1.

2 Related Work

2.1 Pruning Methods are a technique for compressing neural networks which first used a criteria based on the Hessian of the loss function [26, 34] to remove weights. Recent work also explored pruning individual weights based on their overall contribution to the loss [35, 55] and the magnitude based criteria $|w_j|_1$ where w_j is a weight parameter of the network [24, 25, 45]. These networks are initialized based on weights from the first iteration requiring training until full convergence of a full model.

Recent work referred to as the lottery ticket hypothesis (LTH) [19, 63] explored the magnitude criteria and demonstrated small subnetworks are trainable from scratch. Their approach was to first train a randomly initialized over-parameterized network, threshold small weights to zero, then re-initialize the non-zero weights to the same initialization as the over-parameterized network and train only the non-zero weights. This procedure determined that the individual weights are important and not the final weight values from the first stage of training.

2.2 Learning Masks and Weights is a one-stage procedure for learning sparse neural networks through learning a binary mask over the network’s parameters. This pruning problem is formulated as

$$(2.1) \quad Q(W, M|X, y) = \mathcal{L}(h(M) \odot W|X, y) + \xi\Omega(M),$$

where $\Omega(\cdot)$ is a penalty function according to some pre-specified criteria, \mathcal{L} is the standard loss function e.g.

cross entropy for classification, $W = [w_1, w_2, \dots, w_p]$ are the model parameters, M are additional trainable parameters, $h(M)$ is a pre-specified mask function $h : \mathbb{R} \rightarrow \{0, 1\}$, ξ is a non-negative hyperparameter controlling the trade-off between the loss and penalty, and in some cases additional penalties might be applied to W . Numerous works suggest different approaches for selecting the mask function h [4, 32, 37, 48, 55, 58]. Other works explore a Bayesian model for the mask formulation [30, 40] which we explore in Section 3.1 where we discuss point mass priors for inducing sparsity in Bayesian hierarchical models. While this class of models has optimal frequentist properties, the posterior is computationally intractable in many cases and difficult to optimize, and further does not perform any feature selection of non-zero weights. Although (2.1) appears to be very similar to our objective, we note that the class of estimators our approach is based on and this approach are quite different in how they prune models. We elaborate on this difference in Section 3.2.

2.3 Regularization Methods induce sparsity in deep neural networks using a pre-specified criteria (usually referred to as a penalty). In the regularization setting, we consider the modified loss

$$(2.2) \quad Q(W|X, y) = \mathcal{L}(W|X, y) + \xi\Omega(W),$$

Early works in neural network compression with regularization augment the loss function with a sparsity inducing penalty typically based on the Lasso [50] to attain sparse neural networks and prevent overfitting [9, 11, 29, 56]. More recently, Collins et al. [12] applied L_q norm penalties (also called bridge penalties) to achieve sparse networks with $4X$ memory compression over the original network and a minimal decrease in accuracy on ImageNet [31]. The standard L_q norm penalty is written as $\Omega_q(W) = \left(\sum_{j=1}^p |w_j|^q\right)^{1/q}$ for which the popularly used Lasso $q = 1$ and ridge (weight decay) $q = 2$ penalties are special cases. Other extensions include nonconvex penalties like minimax concave penalty (MCP) [60] and smoothly clipped absolute deviations (SCAD) [16] have also been applied to deep neural networks [53]. Other works also induce sparsity through Bayesian hierarchical models [43, 44, 47, 52]; similarly in Section 4 we discuss sparsity and posterior convergence of the Bayesian hierarchical model corresponding to HALO.

3 Background

In this section, we provide background on sparsity inducing regularization and Bayesian shrinkage estimation, and establish connections between our approach HALO and magnitude pruning strategies through the study of sparsity inducing priors.

3.1 Sparse Penalties We start by recalling the L_0 penalty for learning sparse models

$$(3.3) \quad \Omega_0(W) = \sum_{j=1}^p \mathbb{1}[w_j \neq 0]$$

which induces sparsity by penalizing the number of non-zero entries in W without any further bias on the weights W of the model. However, the penalty is computationally intractable as it is non-differentiable and the learning problem is NP-hard. An alternative to L_0 regularization is L_1 regularization obtained by adding the $\Omega_1(W)$ penalty, its tightest convex relaxation. The associated estimator is called the Lasso estimator [50].

Although the Lasso has strong oracle properties under certain conditions, it is a biased estimator [16]. The Lasso requires a neighborhood stability/strong irrepresentable condition on the design matrix X for the selection consistency [51, 54, 62].

3.1.1 The Weighted Lasso and Pruning One approach to reducing the bias in Lasso is to select a different regularization coefficient for each parameter resulting in the weighted Lasso :

$$(3.4) \quad \Omega_{\text{weighted}}(W) = \sum_{j=1}^p \lambda_j |w_j|,$$

or adaptive Lasso penalty [64] which sets $\lambda_j = \frac{1}{\hat{w}_j}$ where \hat{w}_j is an initial estimate from another run of OLS or Lasso.

A more general form for the adaptive Lasso which extends to other sparsity-inducing penalties and any general loss function $\mathcal{L}(\cdot)$ is known as the local linear approximation algorithm (LLA) which iteratively solves the objective in k iterations:

$$(3.5) \quad W^{(k+1)} = \arg \max_W \left[\mathcal{L}(W) - \sum_{j=1}^p \Omega(w_j^{(k)}) |w_j| \right]$$

where $w_j^{(k)}$ are the weights for the previous iteration of LLA [65]. Note that by running this optimization twice with Ω_1 and thresholding the coefficients based on the first run, we recover magnitude pruning [25].

3.1.2 Nonconvex Penalties An alternative approach is to use a penalty that diminishes in value for large parameter values. These types of penalties are non-convex but have been shown to yield both empirical and theoretical results [53, 60, 65]. Fan and Li [16] proposed a non-convex penalty, smoothly clipped absolute deviation (SCAD) penalty, to remove the bias of the Lasso and proved an oracle property for one of the local minimizers of the resulting penalized loss. Zhang [60] proposed another non-convex penalization approach, minimax concave penalty (MCP):

$$(3.6) \quad \Omega_{MCP}(W; \gamma, \lambda) = \begin{cases} \lambda |w_j| - \frac{w_j^2}{\gamma} & |w_j| \leq \gamma \lambda \\ \frac{\gamma \lambda^2}{2} & \text{else} \end{cases}$$

and proved selection consistency.

It has been shown that for some nonconvex penalty functions such as the SCAD penalty, or MCP that the LLA yields an optimal solution when $k = 1$, and as such nonconvex penalties are a more efficient class of penalties [49, 65]. Further, this class of nonconvex penalties is preferred to other penalties as they have been shown to be the optimal class of penalties for achieving sparsity and unbiasedness of the regression parameter estimates [65].

3.2 Bayesian Hierarchical Priors Bayesian hierarchical models have turned out to be useful modeling and estimation approaches since their model structure allows “borrowing strength” in estimation. This means that the prior affects the posterior distribution by shrinking the estimates towards a central value. From a Bayesian point of view we can consider (2.2) as a log posterior density, and with this interpretation the penalty $\xi \Omega(W)$ can then be identified with a log prior distribution of W . Constructing estimates via optimization of (2.2) then gives a maximum a posteriori (MAP) estimation procedure.

The Lasso consists of a Laplace(λ) prior on model parameters W . Strawderman et al. [49] study the estimator given by (3.6) from a hierarchical Bayes perspective. The intuition is that $\exp\{\Omega_{MCP}(W, \lambda; \gamma)\}$ is a hierarchical prior with the first level being a Laplace(λ) prior on W (as with the Bayesian Lasso) and the second level is a half normal prior on the hyperparameter λ . They further studied the priors of the corresponding hierarchical Bayes procedure as part of a class of scale mixture priors similar to those used in dropout [44] and demonstrated that the MAP estimate for this procedure is equivalent to optimization with the MCP penalty for the linear model [49, Remark 4.3]. In our experiments we denote the MAP estimate that corresponds to MCP as SWS.

An alternative to the scale mixture of normals priors are mixture priors of the form

$$(3.7) \quad p(w) = \zeta g(w) + (1 - \zeta) \delta_0, \quad p(\zeta) = \text{Bern}(\pi)$$

which is a mixture of a point mass at zero and a continuous distribution g , these priors are often referred to as spike and slab priors [42]. Variants of this formulation have been studied recently for pruning deep neural networks where a MAP estimate is approximated by learning a continuous function representing a mask over the weights of the network [4, 32, 37, 40, 48, 55, 58].

The primary drawback of spike and slab priors is that posterior computation is much more demanding than for single component continuous shrinkage priors [46] since sampling of the point mass part of the posterior distribution can entail searching over a enormous set of binary indicators and is not feasible in even moderately large parameter spaces. Additionally this class of priors may not effectively penalize the non-zero parameters in W leading to worse predictive performance over normal scale mixture priors.

4 The Hierarchical Adaptive Lasso (HALO)

Although the MCP has desirable properties among shrinkage estimators, a primary drawback is that all weights $w \geq \gamma\lambda$ of the model are penalized equally. For the standard MCP term these are both hyperparameters of the model which must be provided apriori and directly influence the sparsity of the model, and in the hierarchical model, they are derived from the hierarchical Gamma and truncated normal priors [49]. We extend this model by considering an additional level of hierarchy and by making the penalty adaptive such that each w_j has its own λ_j in the scale mixture of normals representation. We consider a first level Laplace prior and further place a mixing distribution on the λ_j 's. Specifically we define the hierarchical prior as

$$(4.8) \quad p(y|\sigma) = \mathcal{N}(W, \sigma^2 I_p)$$

$$(4.9) \quad p(w_j|\alpha, \sigma) = \text{Laplace}\left(\frac{\sigma}{\alpha}\right)$$

$$(4.10) \quad p(\lambda_j|\eta, \sigma, c) = \text{Gamma}(\eta + 1, c)$$

where $\alpha_j = 1/\lambda_j^\eta$ and $\eta + 1 > 0$. Note that the Laplace distribution can be viewed as a scale mixture of normals with an exponential mixing distribution [3]. The second level Gamma prior mixing distribution on the natural parameter of the exponential is related to the class of the exponential-gamma prior distributions developed in [5, 23]. This additional level in the hierarchy is similar to the Horseshoe+ prior which consists of two positive Cauchy distributions [6], and is in contrast to the single level mixture of normals prior used for dropout in Table 1 of [44]. The additional level of the hierarchy in (4.11) allows for additional shrinkage and sparsity over the simpler penalties such as SWS.

Estimation and computation of the posterior distribution for this model can be difficult especially for neural networks with millions of parameters. Instead, by denoting $\alpha_j = h(\lambda_j)$, we obtain a generalized MAP estimate for this model:

$$(4.11) \quad \Omega(W, \lambda; \psi, \xi) = \xi \sum_{j=1}^p h(\lambda_j) |w_j| + \psi \sum_{j=1}^p |\lambda_j|.$$

where $h(\cdot)$ is a positive function for a generalized version of the penalty. We call (4.11) the Hierarchical Adaptive Lasso (HALO) penalty since the hierarchical and adaptive penalty places an additional L_1 norm on the regularization coefficients λ_j . We will call the prior defined by (4.8) - (4.10) the HALO prior. For the MAP estimate both λ and W are trainable parameters in the optimization allowing for learning of the appropriate amount of shrinkage and the weights of the model.

In our experiments, we set $h(\lambda) = 1/\lambda^2$ so that $h(x) \rightarrow \infty$ as $x \rightarrow 0$; this combined with the L_1 penalty on λ_j encourages selective shrinkage of the weights where important weights remain unregularized, and makes HALO a monotonic penalty [7, 18]. This is more flexible than adaptive Lasso methods which fix regularization coefficients each iteration. We modify the SWS penalty to have the same functional penalty as well, and in Section 7.1.1, we explore and suggest alternatives for $h(\cdot)$. Additionally the theorem below gives conditions under which using HALO in (2.2) is convex. A proof of Theorem 1 is provided in Section 7.2.

THEOREM 4.1. *Consider the objective for the penalized linear model*

$$L(W, \lambda) = L(W) + \Omega(W, \lambda; \psi, \xi) \\ = \|y - \sum_{j=1}^p x_j w_j\|^2 + \xi \sum_{j=1}^p \frac{1}{\lambda_j^2} |w_j| + \psi \sum_{j=1}^p |\lambda_j|,$$

and let X be a full rank $n \times p$ matrix with smallest singular value ν . Define

$$\mathbb{R}_{\lambda, W} = \left\{ W, \lambda : 24\nu \frac{\lambda_p^{10}}{|w_p|} \leq \xi^3 \leq 24\nu \frac{\lambda_1^{10}}{|w_1|} \right\}$$

$$\text{with } \frac{\lambda_1^{10}}{|w_1|} \geq \frac{\lambda_2^{10}}{|w_2|} \geq \dots \geq \frac{\lambda_p^{10}}{|w_p|}.$$

Then $\nabla^2 L(W, \lambda) \succ 0$ and $L(W, \lambda)$ is elementwise convex over $\mathbb{R}_{\lambda, W}$.

4.1 Posterior Concentration We will next give a theoretical development for the penalty in (4.11). An assessment of the goodness of an estimator is some measure of center of the posterior distribution, such as the posterior mean or mode. The natural object to use for assessing feature recovery is a credible set that is sufficiently small to be informative, yet not so small that it does not cover the true parameter. The goal is to have a posterior distribution that contracts to its center at the same rate at which the estimator approaches the true parameter value. More formally, the prior gives rise to posterior contraction if the posterior mass of the set $\{w : \|w - w_0\|^2 \geq Mp_n \log(n/p_n)\}$ converges

to zero, where w_0 is the true parameter, $p_n = o(n)$, and M is a constant. The landmark article [20] shows that the posterior concentration property at a particular rate implies the existence of a frequentist estimator that converges at the same rate. Consequently, if the posterior contraction rate is the same as the optimal frequentist estimator, the Bayes procedure also enjoys optimal properties.

For example, consider the Laplace prior, as used in a Bayesian approach to the Lasso, it is well-known that the Laplace distribution with rate parameter λ can be represented as a scale mixture of normals where the mixing density is exponential with parameter $\lambda^2/2$ [3], however Theorem 7 in [10] shows that if the true vector is zero, the posterior concentration rate shown in the full posterior does not shrink at the minimax rate. Theorem 2 gives condition under which the prior induced by the HALO penalty exhibits posterior contraction. The proof is given in Section 7.3.

THEOREM 4.2. *Let $\ell_0(p_n) = \{w : \#(w_i \neq 0) \leq p_n\}$. Define the prior induced by (4.11) as $\pi_{HALO}(w)$ and the corresponding posterior distribution $\pi_{HALO}(w|x)$. Define the event $A(w) = \{w : \|w - w_0\|^2 > M_n p_n \log(n/p_n)\}$. Let $\tau_n = (p_n/n)^\alpha$ with $\alpha > 1$ or $\tau_n = (p_n/n)(\log(n/p_n))^{\frac{1}{2}}$. If $\tau_n \rightarrow 0$, $p_n \rightarrow \infty$ and $p_n = o(n)$ as $n \rightarrow \infty$ then*

$$\sup_{w_0 \in \ell_0(p_n)} \mathbb{E}_{w_0} \pi_{HALO}(A(w)|X) \rightarrow 0$$

for every $M_n \rightarrow 0$.

5 Numerical Results

We present results to motivate and justify the use of HALO as a penalty for learning sparse deep neural networks. To do so, we perform numerical experiments on image recognition datasets where we apply sparsity to the convolutional (feature extraction) layers of the network, which aim to answer the questions

1. Does learning to shrink model parameters improve model performance under highly sparse scenarios?

Section 5.2-5.3: Yes. In nearly all of our experiments on image recognition tasks, the HALO penalty leads to models with higher accuracy than competing methods, and performance is comparable with the full model. Even when the dense model is pre-trained, HALO is still able to prune at least half of the parameters with little reduction in performance.

2. Does the HALO penalty also prevent overfitting in neural networks?

Section 5.4: Yes. On datasets with label noise, HALO learns to ignore irrelevant samples reducing

the generalization gap by over 40% and improving performance by over 10% over standard training with weight decay.

3. Does the HALO penalty induce a particular type of sparsity?

Section 7.6: Yes. The HALO penalty is a monotonic penalty which learns both layer-wise sparsity and low-dimensional feature representations (like PCA or another low-rank factorization of the weight parameters). This means the penalty may also lead to direct computational benefits without directly imposing structured penalization.

5.1 Experimental Setup In our experiments we evaluate the full model trained with weight decay (baseline), several pruning techniques: random initialization pruning [39], lottery ticket hypothesis [19] and GraSP [55], a masked training approach DST [37], and sparsity inducing penalties: Lasso (Ω_1), MCP [60], SWS [49], and the MAP estimate for HALO (4.11) on image recognition tasks for maintaining accuracy while inducing sparsity, and at high sparsity levels¹

We define sparsity to be the ratio of zero weights in the network to the total number of weights in convolutional layers. For all classification results, unless otherwise stated the results represent an average over five runs and the error bars represent one standard deviation. Reported sparsity values are estimated from a single run of the model. Training and regularization hyperparameter details, as well as run-time for all approaches are discussed in 7.4. We use standard benchmark networks and datasets for evaluating pruning methods from [19, 39], which are expanded upon in Section 7.4.

5.2 Image Classification We present accuracy and sparsity ratios for sparse deep neural networks for image classification. Each model contains several fully-connected or convolutional layers for extracting features which we prune, and a final classification layer that outputs the probabilities for each class.

5.2.1 Feedforward Networks on MNIST In the first experiment, we evaluate on the MNIST dataset for digit classification with a fully-connected LeNet-300-100 network, and the convolutional LeNet-5 network. Results benchmarking pruning techniques and penalties are

¹95% sparsity is used for for comparison, particularly [39], and yields competitive performance with the baseline model in most experiments.

Experiment	LeNet-300-100			LeNet-5-Caffe		
	Accuracy	Sparsity	Sparsity at Baseline	Accuracy	Sparsity	Sparsity at Baseline
Baseline	98.57 (± 0.04)	0.6542	0.6542	99.24 (± 0.08)	0.5907	0.5907
Random Init Magnitude Pruning	98.23 (± 0.03)	0.95	0.9	98.91 (± 0.15)	0.95	0.8
Lottery Ticket	98.44 (± 0.13)	0.95	0.95	99.00 (± 0.03)	0.95	0.9
L_1	98.29 (± 0.04)	0.95	0.9	98.96 (± 0.17)	0.95	0.9
SWS	98.17 (± 0.11)	0.95	0.9	98.96 (± 0.15)	0.95	0.9
HALO	<u>98.40</u> (± 0.10)	0.95	0.9	99.12 (± 0.21)	0.95	0.95

Table 1: Accuracy of sparsity-inducing regularization regularization and one-shot magnitude pruning based methods for LeNet-300-100 and LeNet-5-Caffe on MNIST. To obtain the reported sparsity results for the baseline, we threshold values for one of the runs at 0.01.

summarized in Table 1². Overall, all methods perform similarly with the baseline model, and HALO and the LTH perform slightly better on both networks. Most methods are also able to retain the baseline accuracy at over 0.8 sparsity.

5.2.2 Convolutional Networks on CIFAR-10 and CIFAR-100 We additionally evaluate the VGG-like network and ResNet-50 architecture of [39] on the CIFAR-10/100 classification task. Results are summarized in Table 2. For VGG, regularization approaches outperform pruning methods and HALO is able to retain accuracy at high sparsity. On CIFAR-100 in particular, HALO drops performance by only 1% compared with other methods that drop accuracy by 2–3%. On ResNet, all methods drop accuracy, however HALO performs the best at 0.95 sparsity, and achieves similar accuracy to the full model at comparable or higher sparsity ratios. Results at varying levels of sparsity are given in Figure 2 for CIFAR-100. It is important to note, training with HALO always yields a model that attains competitive accuracy with 0.55 or greater sparsity.

5.3 Object Detection We further investigate HALO performance for transfer learning to other image recognition tasks where the back-bone of the network has already been trained to extract features for a similar task. We demonstrate this using the SDS-300 network [38] on the PASCAL VOC object detection task where the goal is to classify objects in an image and estimate bounding box coordinates. In this setting, a VGG network is trained to classify ImageNet, the classification layers are removed, additional convolutional layers for predicting object bounding boxes are defined, and the network is fine-tuned on the Pascal VOC dataset. When training the network with the HALO penalty, the network can be pruned significantly while maintaining similar accuracy

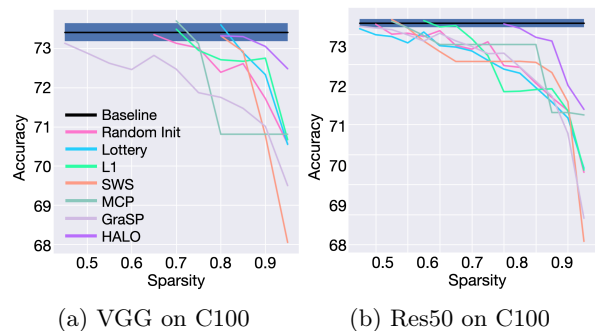


Figure 2: Visualization of test accuracy for various methods at different sparsity ratios. The solid black line represents the mean baseline accuracy over 5 runs and the blue region indicated one standard deviation.

as shown in Figure 3. We find that at 50% sparsity, mean average precision (mAP) drops by 0.013 mAP averaged over 5 runs, and at 70% sparsity, performance only drops by around 0.03 mAP indicating that feature extraction capability from pre-training has been preserved.

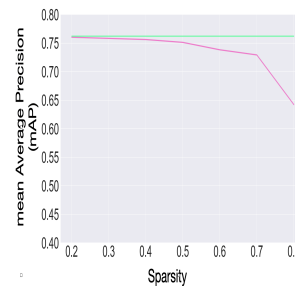


Figure 3: Mean Average Precision of SSD-300 models pruned by HALO (pink) vs. the baseline model (green).

5.4 Regularization for Limiting Overfitting In addition to inducing sparsity and pruning neural network architectures, regularization is a tool for limiting overfitting to noisy data [1, 59]. A common setting where overfitting can occur is in the presence of label

²The reported sparsity is not the highest sparsity ratio attainable by the baseline models, rather a reference that some weights are small enough to threshold. At 0.95 sparsity the full model predicts randomly.

VGG-Like CIFAR-10				ResNet-50 CIFAR-10		
Experiment	Accuracy	Sparsity	Sparsity at Baseline	Accuracy	Sparsity	Sparsity at Baseline
Baseline	93.76 (± 0.20)	0.2176	0.2176	93.48 (± 0.12)	0.1626	0.1626
GraSP	92.52(± 0.10)	0.95	0.9	88.95(± 0.16)	0.95	0.25
Random Init Magnitude Pruning	93.05(± 0.21)	0.95	0.9	88.59(± 0.09)	0.95	0.25
Lottery Ticket	93.18(± 0.12)	0.95	0.9	88.75 (± 0.18)	0.95	0.4
DST	93.27(± 0.13)	0.95	0.92	89.64(± 0.23)	0.95	0.17
L_1	93.51 (± 0.11)	0.95	0.9	89.30 (± 0.46)	0.95	0.6
MCP	92.28(± 0.07)	0.95	0.85	89.54 (± 0.24)	0.95	0.4
SWS	93.50(± 0.15)	0.95	0.9	88.67 (± 0.29)	0.95	0.5
HALO	93.61 (± 0.16)	0.95	0.95	90.71 (± 0.17)	0.95	<u>0.55</u>

VGG-Like C-100				ResNet-50 C100		
Experiment	Accuracy	Sparsity	Sparsity at Baseline	Accuracy	Sparsity	Sparsity at Baseline
Baseline	73.41 (± 0.23)	0.4836	0.4836	70.75 (± 0.28)	0.1018	0.1018
GraSP	69.5(± 0.38)	0.95	0.65	57.76(± 0.39)	0.95	0.25
L_1	70.67 (± 0.24)	0.95	0.7	60.97 (± 0.49)	0.95	0.4
Random Init Magnitude Pruning	70.57 (± 0.37)	0.95	0.65	60.82 (± 0.63)	0.95	0.3
Lottery Ticket	70.55 (± 0.23)	0.95	0.8	61.09 (± 0.35)	0.95	0.25
DST	<u>70.93</u> (± 0.29)	0.95	0.77	62.49(± 0.40)	0.90	0.25
MCP	70.81 (± 0.37)	0.95	0.4	<u>64.51</u> (± 0.43)	0.95	0.25
SWS	68.05 (± 0.28)	0.95	0.8	56.22 (± 1.09)	0.95	<u>0.35</u>
HALO	72.48 (± 0.24)	0.95	0.85	65.01 (± 0.34)	0.95	0.7

Table 2: Accuracy of sparsity-inducing regularization and one-shot magnitude pruning based methods for the VGG-like and ResNet-50 on CIFAR-10 and CIFAR-100. We threshold values at 0.01 for ResNet-50 and 0.001 for VGG-like. Results from baseline and pruning methods at 95% sparsity are taken from [39]. For sparsity at baseline results, we compute the highest sparsity ratio that achieves performance within 0.15 of the baseline.

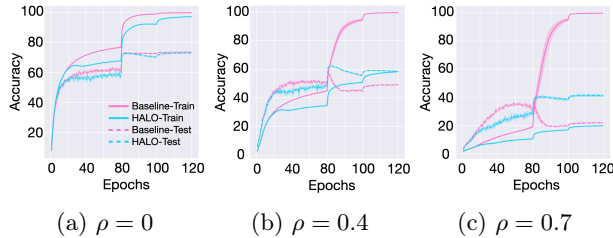


Figure 4: Training and test errors during training for model with the HALO regularizer and baseline model with only weight decay. The mean accuracy over 5 runs and one standard deviation are shown at varying amounts of label noise ρ .

noise where the label of each image in the training set is independently changed to another class label with probability ρ . We implement training of the VGG-like architecture with varying label noise on CIFAR-100. Figure 4 shows the training accuracy for the baseline model approaches 100% while the test error does not when $\rho > 0$. For the VGG-like model trained with the HALO penalty (using suitable hyperparameters to match test accuracy at $\rho = 0$), we find that at $\rho = 0.0$, both train and test curves follow nearly identical patterns, whereas at $\rho = 0.4, 0.7$ the training accuracy does not increase to 100%, but reaches similar accuracy proportional to the clean images. At $\rho = 0.4$, the test error is roughly the

same as the training error indicating a small generalization gap unlike with standard training, while for $\rho = 0.7$ the test accuracy is higher indicating underfitting due to the lack of data. These results indicate HALO can diagnose mis-labeled data in the training set.

5.5 Learning Different Types of Sparsity We have shown that our approach can prune different network architectures in order to achieve small models with little drop in performance. We present results to highlight thorough exploration on the VGG-like architecture that the HALO penalty performs monotonic penalization, learns structured sparsity, and learns low-rank feature representations leading to faster networks with smaller memory footprints. Results are summarized in Figure 5 and expanded upon in 7.6.

6 Conclusion

Over-parameterization is a challenging problem preventing the use of deep neural networks from learning representations in settings with limited computational budgets. In this work, we present HALO, a novel penalty function which when used to train neural networks produces subnetworks which achieve state-of-the-art performance compared with magnitude criteria pruning techniques, without re-training the subnetwork. Our approach has several benefits. It is simple to implement and does not require storing model weights or re-training

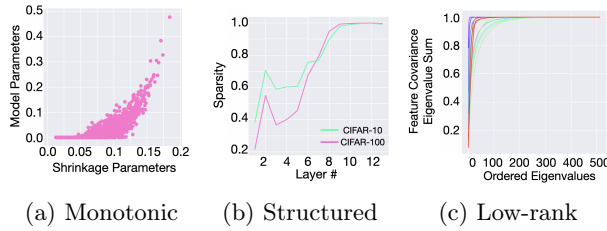


Figure 5: Different types of sparsity learned by HALO. (a) A random sample of 10,000 regularization coefficients and weight parameters illustrating a monotonically increasing trend. (b) Sparsity by layer for CIFAR-10/0 indicating entire layers can be pruned (c) Normalized cumulative sum of eigenvalues of the output covariance matrix indicating a small number of important features. Colors range from violet to red indicate layer number from low to high respectively.

unlike other network pruning methods. Although we only demonstrated results for image recognition, our approach can be combined with other loss functions and is not limited to classification, and is model agnostic. We believe that this work is one step towards creating penalty functions that can be applied to sparsify any model without performance degradation. Further research in this area can lead to impressive performance gains in settings with limited computational resources, and towards a better understanding of the rich feature representations learned by neural networks.

Acknowledgments

We thank Ben Baer for his helpful advice and discussions regarding the LLA algorithm and one-step estimators in Section 3.1, as well as general pointers for optimization with sparsity-inducing penalties and shrinkage priors. Wells’ research supported by NIH grant R01GM135926.

References

- [1] Subutai Ahmad and Luiz Scheinkman. How can we be so dense? the benefits of using highly sparse representations. *arXiv*, 2019.
- [2] Jose M Alvarez and Mathieu Salzmann. Compression-aware training of deep networks. In *Advances in Neural Information Processing Systems*, pages 856–867, 2017.
- [3] Artin Armagan, Merlise Clyde, and David B Dunson. Generalized beta mixtures of gaussians. In *Advances in neural information processing systems*, pages 523–531, 2011.
- [4] Kambiz Azarian, Yash Bhargat, Jinwon Lee, and Tijmen Blankevoort. Learned threshold pruning. *arXiv*, 2020.
- [5] José M Bernardo and Adrian FM Smith. *Bayesian theory*, volume 405. John Wiley & Sons, 2009.
- [6] Anindya Bhadra, Jyotishka Datta, Nicholas G Polson, Brandon Willard, et al. The horseshoe+ estimator of ultra-sparse signals. *Bayesian Analysis*, 12(4):1105–1131, 2017.
- [7] Malgorzata Bogdan, Ewout van den Berg, Weijie Su, and Emmanuel Candes. Statistical estimation and testing via the sorted l1 norm. *arXiv*, 2013.
- [8] Patrick Breheny and Jian Huang. Penalized methods for bi-level variable selection. *Statistics and its interface*, 2(3):369, 2009.
- [9] Miguel A Carreira-Perpinán and Yerlan Idelbayev. “learning-compression” algorithms for neural net pruning. In *Proceedings of the IEEE Conference on Computer Vision and Pattern Recognition*, pages 8532–8541, 2018.
- [10] Ismaël Castillo, Johannes Schmidt-Hieber, Aad Van der Vaart, et al. Bayesian linear regression with sparse priors. *The Annals of Statistics*, 43(5):1986–2018, 2015.
- [11] Yves Chauvin. A back-propagation algorithm with optimal use of hidden units. In *Advances in neural information processing systems*, pages 519–526, 1989.
- [12] Maxwell D Collins and Pushmeet Kohli. Memory bounded deep convolutional networks. *arXiv*, 2014.
- [13] Xavier Suau Cuadros, Luca Zappella, and Nicholas Apostoloff. Filter distillation for network compression. March 2020.
- [14] Jacob Devlin, Ming-Wei Chang, Kenton Lee, and Kristina Toutanova. Bert: Pre-training of deep bidirectional transformers for language understanding. *arXiv*, 2018.
- [15] Andre Esteva, Alexandre Robicquet, Bharath Ramsundar, Volodymyr Kuleshov, Mark DePristo, Katherine Chou, Claire Cui, Greg Corrado, Sebastian Thrun, and Jeff Dean. A guide to deep learning in healthcare. *Nature medicine*, 25(1):24–29, 2019.
- [16] Jianqing Fan and Runze Li. Variable selection via nonconcave penalized likelihood and its oracle properties. *Journal of the American statistical Association*, 96(456):1348–1360, 2001.
- [17] Ky Fan. On a theorem of weyl concerning eigenvalues of linear transformations i. *Proceedings of the National Academy of Sciences of the United States of America*, 35(11):652, 1949.
- [18] Long Feng, Cun-Hui Zhang, et al. Sorted concave penalized regression. *The Annals of Statistics*, 47(6):3069–3098, 2019.
- [19] Jonathan Frankle and Michael Carbin. The lottery ticket hypothesis: Finding sparse, trainable neural networks. *arXiv*, 2018.
- [20] Subhashis Ghosal, Jayanta K Ghosh, Aad W Van Der Vaart, et al. Convergence rates of posterior distributions. *Annals of Statistics*, 28(2):500–531, 2000.
- [21] Prasenjit Ghosh and Arijit Chakrabarti. Asymptotic optimality of one-group shrinkage priors in sparse high-dimensional problems. *Bayesian Anal.*, 12(4):1133–1161, 12 2017.
- [22] Prasenjit Ghosh, Xueying Tang, Malay Ghosh, Arijit Chakrabarti, et al. Asymptotic properties of bayes

- risk of a general class of shrinkage priors in multiple hypothesis testing under sparsity. *Bayesian Analysis*, 11(3):753–796, 2016.
- [23] JE Griffin and PJ Brown. Alternative prior distributions for variable selection with very many more variables than observations. *University of Kent Technical Report*, 2005.
- [24] Yiwen Guo, Anbang Yao, and Yurong Chen. Dynamic network surgery for efficient dnns. In *Advances in neural information processing systems*, pages 1379–1387, 2016.
- [25] Song Han, Huizi Mao, and William J Dally. Deep compression: Compressing deep neural networks with pruning, trained quantization and huffman coding. *arXiv*, 2015.
- [26] Babak Hassibi, David G Stork, and Gregory J Wolff. Optimal brain surgeon and general network pruning. In *IEEE international conference on neural networks*, pages 293–299. IEEE, 1993.
- [27] Geoffrey Hinton, Li Deng, Dong Yu, George E Dahl, Abdel-rahman Mohamed, Navdeep Jaitly, Andrew Senior, Vincent Vanhoucke, Patrick Nguyen, Tara N Sainath, et al. Deep neural networks for acoustic modeling in speech recognition: The shared views of four research groups. *IEEE Signal processing magazine*, 29(6):82–97, 2012.
- [28] Jian Huang, Patrick Breheny, and Shuangge Ma. A selective review of group selection in high-dimensional models. *Statistical science: a review journal of the Institute of Mathematical Statistics*, 27(4), 2012.
- [29] Masumi Ishikawa. Structural learning with forgetting. *Neural networks*, 9(3):509–521, 1996.
- [30] Yohei Kondo, Shin-ichi Maeda, and Kohei Hayashi. Bayesian masking: Sparse bayesian estimation with weaker shrinkage bias. In *Asian Conference on Machine Learning*, pages 49–64, 2016.
- [31] Alex Krizhevsky, Ilya Sutskever, and Geoffrey E Hinton. Imagenet classification with deep convolutional neural networks. In *Advances in neural information processing systems*, pages 1097–1105, 2012.
- [32] Aditya Kusupati, Vivek Ramanujan, Raghav Somani, Mitchell Wortsman, Prateek Jain, Sham Kakade, and Ali Farhadi. Soft threshold weight reparameterization for learnable sparsity. *arXiv*, 2020.
- [33] Yann LeCun, Yoshua Bengio, and Geoffrey Hinton. Deep learning. *nature*, 521(7553):436–444, 2015.
- [34] Yann LeCun, John S Denker, and Sara A Solla. Optimal brain damage. In *Advances in neural information processing systems*, pages 598–605, 1990.
- [35] Namhoon Lee, Thalaiyasingam Ajanthan, and Philip HS Torr. Snip: Single-shot network pruning based on connection sensitivity. *arXiv*, 2018.
- [36] Hao Li, Asim Kadav, Igor Durdanovic, Hanan Samet, and Hans Peter Graf. Pruning filters for efficient convnets. *arXiv*, 2016.
- [37] Junjie Liu, Zhe Xu, Runbin Shi, Ray CC Cheung, and Hayden KH So. Dynamic sparse training: Find efficient sparse network from scratch with trainable masked layers. *arXiv*, 2020.
- [38] Wei Liu, Dragomir Anguelov, Dumitru Erhan, Christian Szegedy, Scott Reed, Cheng-Yang Fu, and Alexander C Berg. Ssd: Single shot multibox detector. In *European conference on computer vision*, pages 21–37. Springer, 2016.
- [39] Zhuang Liu, Mingjie Sun, Tinghui Zhou, Gao Huang, and Trevor Darrell. Rethinking the value of network pruning. *arXiv*, 2018.
- [40] Christos Louizos, Max Welling, and Diederik P Kingma. Learning sparse neural networks through l_0 regularization. *arXiv*, 2017.
- [41] Eran Malach, Gilad Yehudai, Shai Shalev-Shwartz, and Ohad Shamir. Proving the lottery ticket hypothesis: Pruning is all you need. *arXiv*, 2020.
- [42] Toby J Mitchell and John J Beauchamp. Bayesian variable selection in linear regression. *Journal of the american statistical association*, 83(404):1023–1032, 1988.
- [43] Dmitry Molchanov, Arsenii Ashukha, and Dmitry Vetrov. Variational dropout sparsifies deep neural networks. In *Proceedings of the 34th International Conference on Machine Learning-Volume 70*, pages 2498–2507. JMLR. org, 2017.
- [44] Eric Nalisnick, José Miguel Hernández-Lobato, and Padhraic Smyth. Dropout as a structured shrinkage prior. *arXiv*, 2018.
- [45] Sharan Narang, Erich Elsen, Gregory Diamos, and Shubho Sengupta. Exploring sparsity in recurrent neural networks. *arXiv*, 2017.
- [46] Juho Piironen and Aki Vehtari. Sparsity information and regularization in the horseshoe and other shrinkage priors. *Electronic Journal of Statistics*, 11, 07 2017.
- [47] Nicholas G Polson and Veronika Ročková. Posterior concentration for sparse deep learning. In *Advances in Neural Information Processing Systems*, pages 930–941, 2018.
- [48] Pedro Savarese, Hugo Silva, and Michael Maire. Winning the lottery with continuous sparsification. *arXiv*, 2019.
- [49] Robert L Strawderman, Martin T Wells, Elizabeth D Schifano, et al. Hierarchical bayes, maximum a posteriori estimators, and minimax concave penalized likelihood estimation. *Electronic Journal of Statistics*, 7:973–990, 2013.
- [50] Robert Tibshirani. Regression shrinkage and selection via the lasso. *Journal of the Royal Statistical Society: Series B (Methodological)*, 58(1):267–288, 1996.
- [51] Joel A Tropp. Just relax: Convex programming methods for identifying sparse signals in noise. *IEEE transactions on information theory*, 52(3):1030–1051, 2006.
- [52] Karen Ullrich, Edward Meeds, and Max Welling. Soft weight-sharing for neural network compression. *arXiv*, 2017.
- [53] Sujit Vettam and Majnu John. Regularized deep learning with a non-convex penalty. *arXiv*, 2019.
- [54] Martin J Wainwright. Sharp thresholds for high-dimensional and noisy sparsity recovery using ℓ_1 -

- constrained quadratic programming (lasso). *IEEE transactions on information theory*, 55(5):2183–2202, 2009.
- [55] Chaoqi Wang, Guodong Zhang, and Roger Grosse. Picking winning tickets before training by preserving gradient flow. *arXiv*, 2020.
- [56] Andreas S Weigend, David E Rumelhart, and Bernardo A Huberman. Generalization by weight-elimination with application to forecasting. In *Advances in neural information processing systems*, pages 875–882, 1991.
- [57] Wei Wen, Cong Xu, Chunpeng Wu, Yandan Wang, Yiran Chen, and Hai Li. Coordinating filters for faster deep neural networks. In *Proceedings of the IEEE International Conference on Computer Vision*, pages 658–666, 2017.
- [58] Xia Xiao, Zigeng Wang, and Sanguthevar Rajasekaran. Autoprune: Automatic network pruning by regularizing auxiliary parameters. In *Advances in Neural Information Processing Systems*, pages 13681–13691, 2019.
- [59] Chiyuan Zhang, Samy Bengio, Moritz Hardt, Benjamin Recht, and Oriol Vinyals. Understanding deep learning requires rethinking generalization. *arXiv*, 2016.
- [60] Cun-Hui Zhang et al. Nearly unbiased variable selection under minimax concave penalty. *The Annals of statistics*, 38(2):894–942, 2010.
- [61] Dejiao Zhang, Haozhu Wang, Mario Figueiredo, and Laura Balzano. Learning to share: Simultaneous parameter tying and sparsification in deep learning. 2018.
- [62] Peng Zhao and Bin Yu. On model selection consistency of lasso. *Journal of Machine learning research*, 7(Nov):2541–2563, 2006.
- [63] Hattie Zhou, Janice Lan, Rosanne Liu, and Jason Yosinski. Deconstructing lottery tickets: Zeros, signs, and the supermask. pages 3592–3602, 2019.
- [64] Hui Zou. The adaptive lasso and its oracle properties. *Journal of the American Statistical Association*, 101(476):1418–1429, 2006.
- [65] Hui Zou and Runze Li. One-step sparse estimates in nonconcave penalized likelihood models. *Annals of statistics*, 36(4):1509, 2008.

7 Appendix

7.1 Generalizations of HALO

7.1.1 Other choices of $h(\mathbf{x})$ We introduced the HALO penalty and in our experiments we consider $h(x) = \frac{1}{x^2}$ to enforce $h(x) \rightarrow \infty$ as $x \rightarrow 0$. We found that this combined with the L_1 penalty on λ_j encourages selective shrinkage of the weights where important weights remain unregularized. Using $h(x) = \frac{1}{x^k}$ when $k > 0$ is favorable because $h(x) \rightarrow 0$ and ∞ as $x \rightarrow \infty$ and 0 respectively. With this choice of $h(x)$ our penalty is a flexible variant of the adaptive penalties such as magnitude pruning or the relaxed

Lasso because the regularization coefficients in these approaches (regularization coefficients are pre-specified as either zero or infinity) are the limit of those learned by HALO. However in some cases it may not be favorable to use a sharp penalty on the regularization coefficients since this may lead to over-sparsification of the weights.

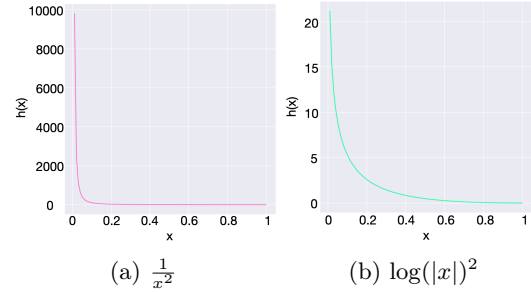


Figure 6: Comparing different choices of $h(x)$ for HALO.

As an alternative, we investigate $h(x) = \log(|x|)^2$. Figure 6 highlights the key difference: $\log(|x|)^2$ approaches infinity at a much slower rate over $\frac{1}{x^2}$, thus inducing less shrinkage of small coefficients. Another difference is that for $x > 1$, $\log(|x|)^2$ is an increasing function. This means that increasing λ will also penalize weights, although this will rarely happen since the L_1 penalty acts to shrink the λ s as much as possible. On experiments with VGG-16 on CIFAR-100 we obtain comparable accuracy of 72.36 ± 0.22 for VGG-like on CIFAR-100. This is similar to the performance with $h(x) = \frac{1}{x^2}$ (72.48 ± 0.24).

Although we have not fully explored the range of possible functions for HALO, we believe that the choice of $h(x)$ will be data, model and application dependent. A choice of $h(x)$ such that $h(x) \rightarrow \infty$ as $x \rightarrow 0$ and 0 as $x \rightarrow \infty$ will lead to a soft-thresholding variant of the common magnitude pruning approaches, while a choice of $h(x) \rightarrow \infty$ as $x \rightarrow 0$ and ∞ will impose additional restraints on weight magnitudes (favoring medium magnitude weights). Still there are many other functions we can explore in future work including piecewise functions that have different behaviors for large and small weights, or those which lead to other penalty behaviors such as sorted penalties [7, 18] which penalize larger weights more strongly.

7.1.2 Structured HALO We demonstrate that HALO learns efficient sparse architectures in performing effective dimensionality reduction of the features and nearly sparsifying entire layers. However, HALO is not a structured penalty and it is not guaranteed to enforce sparsity at a group level. While prior work [41] shows that subnetworks pruned at the neuron-level are unable

to attain performance equivalent to trained networks, whereas subnetworks pruned at the weight-level can, in some cases structured sparsity may be more desirable. We propose a natural extension of HALO to structured penalization for deep neural networks. One possible version of a structured HALO (SHALO) penalty is based on the composite penalty framework proposed in [8]

$$\Omega_C = \Omega_O \left(\sum_{j=1}^{p_g} \Omega_I(|w_{gj}|) \right),$$

where Ω_O is some out penalty applied to the sum of inner penalties Ω_I and w_{gj} is the j th member of the g th group. This framework is general for group penalties and includes both the group bridge penalty and group Lasso [28]. The partial derivative with respect to the gj th weight is

$$\frac{\partial \Omega_C}{\partial w_{gj}} = \partial \Omega_O \left(\sum_{j=1}^{p_g} \Omega_I(|w_{gj}|) \right) \partial \Omega_I(|w_{gj}|)$$

and this approach can be applied with the HALO penalty for learning structured sparsity in deep neural networks. We suggest two approaches for extending HALO

1. Apply a Lasso penalty for the inner penalty and HALO for the outer penalty:

$$\Omega_{\text{SHALO}} = \xi \sum_{g=1}^G h(\lambda_g) \sum_{j=1}^{p_g} |w_{gj}| + \psi \sum_{g=1}^G |\lambda_g|,$$

which learns regularization coefficients for controlling groups of weights only.

2. Apply the HALO penalty for both the inner and outer penalty:

$$\Omega_{\text{SHALO}} = \xi \sum_{g=1}^G h(\lambda_g) \sum_{j=1}^{p_g} \Omega_{\text{HALO}}(\mathbf{w}_g) + \psi \sum_{g=1}^G |\lambda_g|,$$

where \mathbf{w}_g is the vector of all weights in the g th group. This penalty will learn regularization coefficients group-wise and for individual weights.

In future work, we hope to consider these penalties and other structured variants for learning more efficient sparse networks.

7.2 Theorem 1: Convexity of HALO in the Linear Model We demonstrate that for the standard linear model, the loss function with the HALO penalty is convex.

LEMMA 7.1. *For any symmetric matrix*

$$M = \begin{bmatrix} A & B \\ B & C \end{bmatrix}$$

if A is invertible, then $M \succ 0$ iff $A \succ 0$, and $C - B^T A^{-1} B \succ 0$.

We invoke Lemma 1 to show convexity in both W and $\lambda = [\lambda_1, \lambda_2, \dots, \lambda_p]$:

Proof. First, note that $\nabla^2 L(W, \lambda)$ is symmetric and can be written as a block matrix since

$$\begin{aligned} \nabla^2 L(W, \lambda) &= \begin{bmatrix} A & B \\ B & C \end{bmatrix} \\ &= \begin{bmatrix} \text{diag}(\frac{6\xi w_k}{\lambda_k^4}) & \text{diag}(\pm \frac{2\xi}{\lambda_k^3}) \\ \text{diag}(\pm \frac{2\xi}{\lambda_k^3}) & X^T X \end{bmatrix} \end{aligned}$$

Second, since A is a diagonal matrix with positive values along the diagonal, A is both invertible and $A \succ 0$. Consider the expression

$$\Lambda = C - B^T A^{-1} B.$$

Note that if X is full rank, then the smallest eigenvalue of $X^T X$ is $\nu > 0$. Further, the eigenvalues of $B^T A^{-1} B$ are

$$\rho_k = \frac{4\xi^2}{\lambda_k^6} \cdot \frac{6\xi |w_k|}{\lambda_k^4}.$$

Then, By Weyl's theorem [17],

$$\nu - \rho_p \leq \mu_p \leq \nu - \rho_1$$

where μ_p is the smallest eigenvalue of Λ , ρ_p is the smallest eigenvalue of $B^T A^{-1} B$, and ρ_1 is the largest. Then, since

$$24\nu \frac{\lambda_p^{10}}{|w_p|} \leq \xi^3 \leq 24\nu \frac{\lambda_1^{10}}{|w_1|}$$

we have

$$0 \leq \nu - \rho_p \leq \mu_p \leq \nu - \rho_1$$

and $\Lambda \succ 0$.

□

Remark: Note that the conditions of the proof do not depend on ψ . While we believe ψ cannot be entirely disregarded, based on the above theorem and empirically, HALO has only one key hyperparameter ξ rather than two.

7.3 Theorem 2: Posterior Contraction of HALO We demonstrate that the posterior contraction property holds by satisfying the conditions of [21, Theorem 4]. The results in [21] use the notion of slowly-varying functions and their general theorem depends on the fact that the hierarchical prior can be represented in terms of such a function. [21] assume the following two conditions hold for some slow-varying function $L(\cdot)$:

1. $\lim_{t \rightarrow \infty} L(t) \in (0, \infty)$ and
2. there exists some $0 < M < \infty$ such that $\sup_{t \in (0, \infty)} L(t) < M$.

Specifically, in [21] it is shown that a large class of mixture of normal priors, specifically normal-exponential-gamma priors, are in the family of “Three Parameter Beta” (TPB) priors [3]. Membership in the TPB family of priors implies the normal-exponential-gamma prior can be represented by a function proportional to $w_i^{-\beta-1} L(w_i)$ for some $\beta > 0$ and a slowly varying function $L(\cdot)$ satisfying the assumptions of Theorem 2 [22]. With the prior having the representation connected to the slowly vary function L , it is shown that the normal-exponential-gamma prior has the posterior contraction property.

For HALO, π_{HALO} we can demonstrate posterior contraction because the tail properties of π_{HALO} are the same as those of the normal-exponential-gamma prior. Therefore in terms of the tail behavior, it follows that $\pi_{HALO} \propto w_i^{-\beta-1} \tilde{L}(w_i)$ for some $\beta > 0$ and \tilde{L} satisfying the conditions of Theorem 2. Consequently, the posterior contraction of π_{HALO} follows directly from [21, Theorem 4].

7.4 Training Configurations We use the standard train/test split for the MNIST digits dataset containing 60,000 training images and 10,000 test images, and CIFAR-10/0 datasets which contain 50,000 training images and 10,000 test images available from the torchvision dataloaders³. For the Pascal VOC dataset, we train using the trainset from Pascal 2007 and Pascal 2012, and test on the Pascal 2007 testset.

We train all models using SGD with a momentum of $\gamma = 0.9$ and weight decay. For MNIST, we use a batch size of 100 and train with an initial learning rate of 0.1 decaying by 0.1 at every 25k batches for 250 epochs, and use weight decay of 0.0005. For CIFAR-10/100 we use a batch size of 64, and train with an initial learning rate of 0.1 decaying by 0.1 at the 80th and 120th epochs for 160 epochs. We set the weight decay parameter to be 0.0001. For CIFAR-10/100 experiments, we use standard data augmentations (random horizontal flip, translation by 4 pixels). For Pascal VOC, we train with a batch size of 32 and weight decay 0.0005 for 120,000 steps at a learning rate of 0.001 decreasing the learning rate at 80,000 and 100,000 steps. Regularization coefficients are initialized at one for all λ_j and have their own optimizer but follow the same decay rate. This also reduces our approach to Lasso for the first batch.

³<https://pytorch.org/docs/stable/torchvision/datasets.html>

7.5 Parameter Robustness We plot accuracy of one model run according to different values of ξ and ψ . In our experiments, we set $\xi = \psi$ in order to eliminate the advantage of our approach having an extra hyperparameter over the L_1 penalty and MCP which does not have the hierarchical term. In our main results, we report accuracy for each regularization approach based on the best performing regularization hyperparameters, although we note that for HALO, there are often a few hyperparameter choices which perform comparably or better than competing methods. Results for CIFAR-100 are given in Figure 7; results are similar for other datasets and networks. Results indicate that HALO has a wider range of “acceptable” parameter values while attaining higher accuracy.

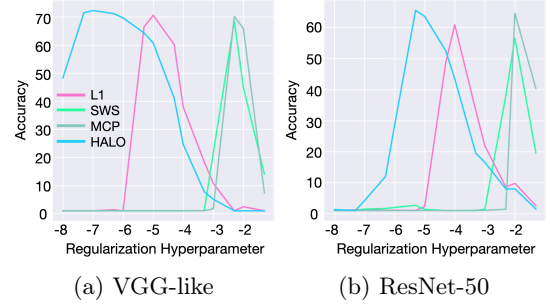


Figure 7: Visualization of accuracy of VGG-like and ResNet-50 architectures at 0.95 sparsity across different values of ξ and ψ on CIFAR-100. On the x-axis we plot the regularization coefficients on a \log_{10} scale.

7.6 Learning Different Types of Sparsity We have shown that our approach can prune network architectures in order to achieve small models with little drop in performance. We further discuss the type of sparsity learned through the HALO penalty. In particular, we highlight that the HALO penalty performs monotonic penalization, learns structured sparsity, and learns low-rank feature representations.

Approximately Structured Penalization: To take advantage of unstructured sparsity, sparse libraries or special hardware is required to deploy such networks, and recent work has aimed at pruning layers, filters, or channels of the network [2, 36, 57, 61]. We note that while it is not guaranteed for HALO to learn sparse group representations, our procedure learns to nearly sparsify complete layers yielding more efficient networks without needing sparse libraries or other mechanisms as shown in the main paper. We find that for early layers (before layer 5) the sparsity ratio is low, for middle layers (layers 5-8) there is a sharp increase in the sparsity level, and above layer 8, layers are near fully sparse. Interestingly

layer 2 exhibits a high amount of sparsity (approximately 70%) on CIFAR-100, and the sparsity seems to exhibit a pattern every few layers. The pattern appears to arise from the structure of the VGG architectures which separate convolutional layers with max-pooling layers with large jumps or discontinuities occurring after max-pooling layers.

Low-Rank Penalization: We additionally plot the normalized cumulative sum of the eigenvalues of the covariance matrix generated from the outputs of each convolutional layer, which reflects the dimensionality of the output feature space. For the CIFAR-100 training set there is a sharp trend which plateaus at 1 after only very few eigenvalues. This indicates that the covariance matrix of the outputs is low-rank, and that the HALO penalty learns a model producing a low-dimensional representation of the feature spaces, much as other low-rank factorization approaches which might apply a low-rank matrix factorization (like PCA) to intermediate layers. Although untested, this type of representation is also learned to de-correlate and prune filters in [13]. We note that as with the structured penalization, the intermediate layers have the largest effective dimensionality. Along with the increase in sparsity during the intermediate layers, this may imply that the middle layers are the most feature-rich for image classification, and are an important subject for future work.

Additional sparsity plots for ResNet-50 on CIFAR-100 are provided in Figure 8. A key difference with those of VGG is that the large drops in sparsity per layer are from the downsample layers at the end of each block in ResNet which lower the width and height and increase the number of channels.

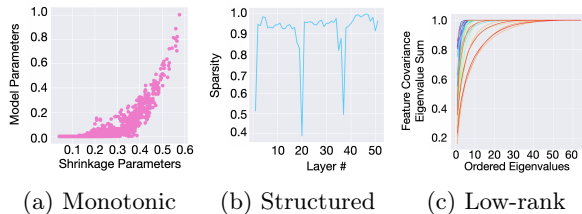


Figure 8: Different types of penalties learned by HALO for ResNet-50 on CIFAR-100 at 0.95 sparsity. (a) A random sample of 10,000 regularization coefficients and weight parameters illustrating a monotonically increasing trend. (b) Sparsity by layer for CIFAR-10/0 indicating entire layers are sparse (c) Normalized cumulative sum of eigenvalues of the output covariance matrix indicating a small number of important features. Colors ranging from violet to red indicate layer number from low to high.

We additionally provide sparsity plots for VGG and ResNet-50 when the sparsity is below 0.95 and the accuracy is maintained. The characteristics of sparsity are similar to those at the higher 0.95 sparsity level, which means that these are properties achievable with minimal drop in performance as seen in Figures 9 and 10.

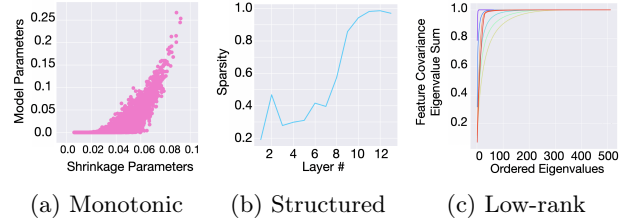


Figure 9: Different types of penalties learned by HALO for VGG-like on CIFAR-100 at 0.85 sparsity.

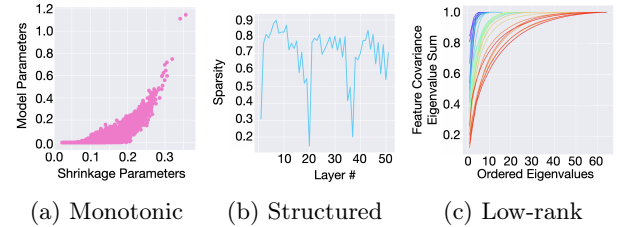


Figure 10: Different types of penalties learned by HALO for ResNet-50 on CIFAR-100 at 0.7 sparsity.

7.7 Training Time We summarize training time reported as the number of seconds taken to train a VGG-like network on CIFAR-100 with each penalized training approach in Table 3. We find that regularization approaches are slower for a single epoch, however pruning methods require two or more stages of training and in our experiments require double the number of epochs for training.

Method	Train Time
Baseline	19.07 (± 0.24)
L_1	23.98 (± 0.54)
SWS	25.90 (± 0.37)
HALO	31.63 (± 0.23)

Table 3: Average training time for a single epoch using a penalty over 5 runs with standard deviation.

7.8 Sparsity During Training We plot the amount of sparsity in the model during training for both the VGG-like architecture and ResNet architecture

(Figure 11) by counting the number of parameters in the model which are smaller in magnitude than the 95th percentile weight from a fully-trained network trained with the same penalty. For both architectures, we find that adaptive penalties pushes coefficients to zero at a slower rate than the non-adaptive penalty. The threshold for the weights trained with adaptive penalty in both architectures is also smaller than the threshold for the L_1 penalty as seen in the lower sparsity at initial epoch indicating that the weights are further shrunk to 0 over the L_1 penalty.

In contrast to the L_1 and HALO penalties, on VGG, the SWS penalty penalizes relatively late in the training phase and attains a small threshold, several orders of magnitude smaller than the L_1 and HALO penalties indicating it has set a majority of the weights to nearly zero at the end of training.

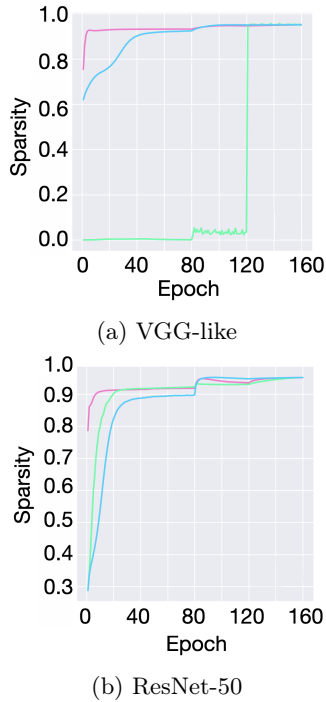


Figure 11: Amount of sparsity during training on CIFAR-100. Pink: L_1 , Green: SWS, Blue: HALO

7.9 Sparsity Overlap We investigate how similar the learned parameters are to one another over multiple runs of HALO and summarizes the results in Figure 12. The sparsity overlap (SO) is computed as the Jacard similarity of zero weights in two models; that is, let \mathcal{A} be the set of zero weights for model A and \mathcal{B} be the set of weights for model B . Then the sparsity overlap for model A and B is defined as $SO = \frac{\mathcal{A} \cap \mathcal{B}}{\mathcal{A} \cup \mathcal{B}}$.

The shape of the sparsity overlap in Figure 12 follows that of the structured penalization, which means that the higher the level of sparsity in a layer the higher the percentage overlap of sparsity across multiple runs of HALO. This is straightforward for the highly sparse layers. For the less sparse layers, this means that there are multiple winning tickets, which can be expected due the large number of weights.

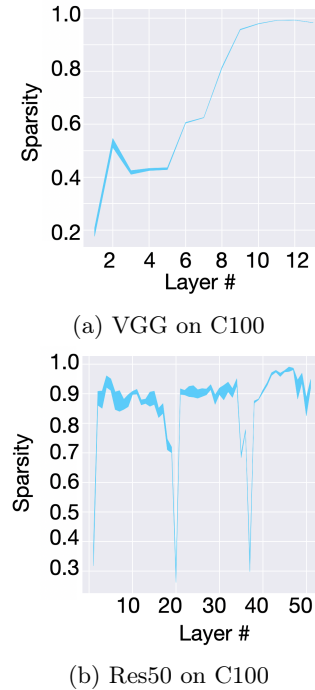


Figure 12: Sparsity overlap (SO) averaged over four runs for different HALO models compared with one another.